A new type of Ca^{2+} channel blocker that targets Ca^{2+} sensors and prevents Ca^{2+}-mediated apoptosis

MICHAEL K. MANION, ZHENGCHANG SU, MATTEO VILLAIN,[1] AND J. EDWIN BLALOCK[2]

University of Alabama at Birmingham, Department of Physiology and Biophysics, Birmingham, Alabama 35294, USA

ABSTRACT **Calmodulin (CaM), as well as other Ca^{2+} binding motifs (i.e., EF hands), have been demonstrated to be Ca^{2+} sensors for several ion channel types, usually resulting in an inactivation in a negative feedback manner. This provides a novel target for the regulation of such channels. We have designed peptides that interact with EF hands of CaM in a specific and productive manner. Here we have examined whether these peptides block certain Ca^{2+}-permeant channels and inhibit biological activity that is dependent on the influx of Ca^{2+}. We found that these peptides are able to enter the cell and directly, as well as indirectly (through CaM), block the activity of glutamate receptor channels in cultured neocortical neurons and a nonselective cation channel in Jurkat T cells that is activated by HIV-1 gp120. As a consequence, apoptosis mediated by an influx of Ca^{2+} through these channels was also dose-dependently inhibited by these novel peptides. Thus, this new type of Ca^{2+} channel blocker may have utility in controlling apoptosis due to HIV infection or neuronal loss due to ischemia.—Manion, M. K., Su, Z., Villain, M., Blalock, J. E. A new type of Ca^{2+} channel blocker that targets Ca^{2+} sensors and prevents Ca^{2+}-mediated apoptosis. *FASEB J.* 14, 1297–1306 (2000)**

Key Words: calmodulin · CALP · Fura-2 · cation channel · complementary peptide · antisense peptide

Apoptosis is a process whereby cells die in a controlled manner, following an intrinsic program. In many instances, Ca^{2+} plays a central role in this process in that the initial stimulus for apoptosis triggers a requisite influx of Ca^{2+} into the cell (1–4). Thus, agents that block Ca^{2+} entry often inhibit apoptosis (5–9). Although such Ca^{2+} channel blockers often act on the channel's pore region or ligand binding site, a new regulatory site representing a potential target for a new generation of Ca^{2+} channel blockers has recently been described. Specifically, certain Ca^{2+} binding motifs, termed EF hands, or binding sites for proteins with EF hands such as calmodulin (CaM) are responsible for inactivating Ca^{2+} channels (10–29). EF hand motifs consist of a helix-loop-helix with the coordination site for Ca^{2+} encompassed by the loop. Consequently, these sites might be exploited to control apoptosis, which is dependent on Ca^{2+} conduction through such channels.

As an approach toward rationally designing molecules that specifically bind the aforementioned Ca^{2+} sensors, we have used the technique of inverted hydropathy (30, 31) to produce a series of peptides, termed calcium-like peptides or CALP (32, 33). These peptides are thought to interact with Ca^{2+} binding motifs as a result of having a complementary surface contour to a stretch of eight amino acids of the loop sequence of EF hands (33). This study presents the biological activity of two such peptides, CALP1 and CALP3. In a recent report we have demonstrated that both of these octameric peptides share similar biochemical activity in that they are able to bind the EF hands of CaM. The peptide/CaM complex in turn was able to activate phosphodiesterase in the absence of Ca^{2+}. These results demonstrated a specific and productive interaction of CALP with the desired target protein. This also suggested the possibility that these peptides might block Ca^{2+}- and CaM-regulated Ca^{2+} channels and consequently inhibit apoptosis, which is dependent on Ca^{2+} entry.

In this report, we describe the ability of CALP to enter cells and directly as well as indirectly via CaM block glutamate receptor channels and a store-operated nonselective cation channel (NSCC). This inactivation is apparently due to a peptide/EF hand interaction involved in regulating such channels. As a consequence, CALP inhibited apoptosis mediated by glutamate as well as HIV-1 gp120. Collectively, these results demonstrate a new type of Ca^{2+} channel blocker that may have utility in controlling apoptosis in diseases such as AIDS or neuronal loss due to ischemia.

[1] Current address: Department of Medicinal Chemistry, University of Geneva, Rue R.M. Servet, Geneva, CH. Switzerland.

[2] Correspondence: University of Alabama at Birmingham, Department of Physiology and Biophysics, McCallum Building, Rm. 898, 1918 University Blvd., Birmingham, Alabama 35294, USA. E-mail: blalock@uab.edu

MATERIALS AND METHODS

Reagents

All peptides used (see **Table 1** for sequences) were synthesized in our laboratory using solid-phase peptide synthesis with Fmoc chemistry and Opfp(*O*-pentafluorophenyl ester) amino acids activated with HOAt (1-hydroxy-7-azabenzotriazole) on a PerSeptive 9050 Peptide synthesizer. All reagents for peptide synthesis were purchased from PerSeptive Biosystems (Framingham, Mass.) unless otherwise mentioned. Preloaded PEG-PS (polyethylene glycol graft polystyrene) resin was used, and all the peptides were purified by reverse phase-high performance liquid chromatography (RP-HPLC) on a Delta Pack C18 300A 30 × 3 id cm column. The purity of the product (always >90%) was checked by RP-HPLC on a Dynamax C18 (300×4.8 id) column with a gradient from 0 to 90% acetonitrile and 0.1% trifluoacetic acid in 40 min. The identities of the peptides were confirmed by TOF-MALDI mass spectrometry (UAB core facility).

Cyclic-CALP3 (Table 1) was synthesized starting from Fmoc-Asp(PEG-PS)-OAl. After amino-terminal Fmoc removal and allyl side chain deprotection with $Pd[(C_6H_5)_3P]_4$ (Fluka, Ronkonkoma, N.Y.), the peptide was cyclized on the support using PyAOP ([7-azabenztriazol-1-yloxytris(pyrrolidino) phosphonium-hexafluorophosphate) and DIPEA (diisopropylethylamine). The cyclization was confirmed by mass spectroscopy.

For F-CALP1 (Table 1) the sequence was extended in the carboxyl-terminal direction with a cysteine. The side chain sulfur was selectively functionalized using fluorescein-5-malemide (Pierce, Rockford, Ill.) at pH 6.5. The final product was purified by RP-HPLC and confirmed by mass spectroscopy.

Peptides were stored as lyophilized 50 μl aliquots of a 5 mM stock at −20°C, reconstituted in MilliQ water before being diluted in buffer or media at final concentrations shown.

Cell culture

Neocortical cultures were made from the frontal cortex of Sprague-Dawley rats (Harlan, Indianapolis, Ind.) taken at embryonic day 18. Briefly, after removal of all surrounding tissue and vasculature, the cortical layer was peeled off and placed in 0.25% trypsin (Gibco BRL, Gaithersburg, Md.) for 10 min at room temperature. This was followed by mechanical dissociation using a graded series of fire-polished Pasteur pipettes. Cells were plated in 96-well culture plates or on 22 mm glass coverslips that had been coated with 1 mg/ml poly-L-lysine (Sigma). The media consists of basal medium Eagle (Gibco-BRL) supplemented with 100 μg/ml penicillin-streptomycin, 2 mM L-glutamine (Cell-Gro), 100 μg/ml Gentamicin sulfate (Sigma), 5% iron-supplemented bovine calf serum (Atlanta Biologicals, Atlanta, Ga.), 5% CPSR-3 (Sigma), and 5 g/l glucose. The media was always warmed to 37°C before adding to the cells. Cells were fed every 5 days by replacing half of the supernatant from each culture well with fresh media. Experiments were conducted between days 8 and 10 in culture.

T cells were isolated from human peripheral blood (American Red Cross, Birmingham, Ala.) first by centrifuging the buffy coat over a layer of Ficoll-Hypaque (using Histopaque 1.077g, Sigma) to remove red blood cells; then white blood cells were passed over a nylon wool column to remove adherent B cells. This procedure yielded a culture that was ~80% T cells as determined by flow cytometry (data not shown).

Both Jurkat E6–1 T cells (American Type Culture Collection, Norcross, Ga.) and T cell-enriched human peripheral blood cells were cultured at 37°C with 5% CO_2 in RPMI media with 10% fetal bovine serum (Atlanta Biologicals), 100 μg/ml Penicillin/streptomycin, (1×) nonessential amino acid solution, 2 mM L-glutamine, 1 mM sodium pyruvate (Cell-Gro, Herndon, Va.), 23.8 mM sodium bicarbonate, 10 mM HEPES (Sigma, St. Louis, Mo.). Jurkat cells were diluted 1:10 in fresh media every 2–3 days.

TABLE 1. *Amino acid sequences of CALP and control peptides*[a]

Name	Sequence
CALP1	VAITVLVK
CALP3	VKFGVGFK
cyclic CALP3	[VKFGVGFKD]
F-CALP1	VAITVLVKC(Fluorescein)
F-MBP	(Fluorescein)CASQKRPSQR

[a] Peptides shown from amino- to carboxy-terminal. Note that although cyclicCALP3 is shown in linear fashion, the line indicates that the amino and carboxy termini are linked. The fluorescein maleimide on F-CALP1 and F-MBP is linked through the sulfhydryl group on the cysteine.

Fluorescent microscopy of F-CALP1-loaded cells

Approximately 50 μM F-CALP1 was added to the culture media and the cells were incubated at room temperature in the dark for 15 min. Then Hoechst 33258 (7.5 μM, Sigma) was added and the cells were incubated for an additional 5 min. This was followed by washing the cells with normal Ringer's solution and fixing for 5 min at room temperature with Bouin's solution (Sigma). The cells were washed again twice with Ringer's solution and mounted on glass slides. Digital images were acquired using an Olympus IX70 digital confocal microscope (Lake Success, N.Y.) equipped with a Sensys 1400 CCD camera (Photonics, Tucson, Ariz.). Image analysis was done using IPLab Spectrum software.

Ca^{2+} imaging using Fura-2

Neuronal cultures made on 22 mm glass coverslips grown in 6-well plates were loaded with 2 μM fura 2-acetoxymethlyester (Molecular Probes, Eugene, Oreg.) in the cell's media at room temperature for 1 h in the dark. This loading was stopped by washing the cells three times in normal Ringer's solution. Cells were allowed to de-esterify for 15 min at room temperature before they were used. Coverslips containing loaded cells were placed in a chamber on the stage of a Nikon Diaphot 200 inverted epifluorescence microscope and visualized using a 40× oil immersion objective. The dye was alternately excited at 340 and 380 nm with a single wavelength monochrometer (Photon Technologies International, South Brunswick, N.J.) and a ratio was obtained every 4 s. The emitted fluorescence above 520 nm was captured by video camera (Hamatsu, Hamal Su City, Japan), then digitized and saved on a personal computer, and analyzed using Image Master software (Photon Technologies International). The ratio of the two images (340/380 nm) was calculated, which is reflective of $[Ca^{2+}]_i$. Glutamate and CALP were added as a bolus to the 1 ml chamber from a 10 mM and 5 mM stock solution, respectively. Ionomycin (10 μM final concentration) was added at the end of each experiment to check for variability and to determine whether the limits of saturation of the Fura-2 had been reached. For each data point, three experiments were done, recording 20 cells from each coverslip. The data are represented as the mean increase in $[Ca^{2+}]_i$ ± SE.

Electrophysiological studies by patch clamping

For recordings on Jurkat cell, we used a conventional whole-cell technique. Briefly, Jurkat E6–1 cells were washed twice with the external solution (see below). The cells were resuspended and allowed to settle on a glass coverslip for 10 min; the unsettled cells were removed by washing the coverslip twice with the external solution. Recording was conducted by using a List EPC-7 patch clamp amplifier (LIST Medical, Darmstadt-Eberstadt, Germany). Pipettes were pulled from KG12 capillaries (World Precision Instrument, Inc., Sarasota, Fla.), Q-Dope coated and fire-polished to produce a tip resistance of 3–5 MΩ in the external solution. Internal solution contained (in mM): 140 CsGlut, 2 $MgCl_2$, 1 $CaCl_2$, 10 EGTA-Cs, 5 HEPES, pH 7.2. The external solution contained (in mM): 131 NMDGCl, 10 $CaCl_2$, 2.2 $MgCl_2$, 5.6 D-glucose, 39 HEPES, pH 7.4. A tip junction potential of +10 mV was not corrected. The capacitative current was compensated. After whole-cell configuration was achieved, the cells were held at 0 mV, and a series of voltage steps from −80 to +80 mV with a 20 mV increment were applied to the cell each minute to measure the current. Currents were sampled at 2 kHz and filtered at 1 kHz by an 8 pole low-pass Bessel filter (Model 900, Frequency device). Drugs were added directly into the chamber.

For cell-attached and inside-out recording of NSCC in Jurkat cells, the pipette contained (in mM): 150 NaCl, 11 $MgCl_2$, 10 HEPES, 5 glucose, pH 7.3 (with NaOH). Bath solution contained (in mM): 150 KCl, 1 $CaCl_2$, 2 $MgCl_2$, 10 EGTA·K, 10 HEPES, pH 7.2 (with KOH). Gp120 (8.3 nM) and CALP1 (120 μM) were added to the bath solution as specified. Holding potential was −80 mV, and the signal was digitized at 20 kHz and recorded by a Sony VCR on a magnetic tape. For analysis and display, the data were resampled at 10 kHz and filtered at 300 Hz by an 8 pole low-pass Bessel filter.

We used a perforated whole-cell technique to record from neurons. The external solution contained (in mM):162 NaCl, 2.4 KCl, 1.3 $CaCl_2$, 10 HEPES, 10 D-glucose, 0.01 glycine (pH 7.4) adjusted with NaOH. Tetrodotoxin (0.5 μM), picrotoxin(50 μM), and strychnine(2 μM) were added to block voltage-gated Na^+ channels, GABA receptor, and glycine receptors, respectively. The pipette solution contained (in mM): 55 CsCl, 70 Cs_2SO_4, 7 $MgCl_2$, 1 $CaCl_2$, 5 D-glucose, 10 HEPES, pH 7.2, adjusted with CsOH. A final concentration of 300 μM amphotericin-B from freshly prepared stock (60 mg/ml in DMSO) was added to the pipette solution. Whole-cell configuration could be achieved within 10 min. Cells were used only if they had series resistance of less than 20MΩ. After whole-cell configuration was achieved, the capacitative currents were compensated and neurons were held at −80 mV. Series resistance compensation was not used. The drugs were delivered to the chamber by a gravity-feeding perfusion system. The solution change was achieved within 1 s as measured by blockage of glutamate current by 200 μM CNQX and 40 μM AP-5. The signals were digitized at 20 kHz and recorded by a VCR (Sony, Tokyo, Japan) on a magnetic tape. For presentation, the signal was resampled at 50 Hz and analyzed using PCLAMP software (Axon Co., Foster City, Calif.).

For cell-attached recordings of the neurons, the pipettes were fabricated the same way as in the whole-cell recording, but with a tip resistance of 1–3 MΩ in the same solution. Neurons were bathed in the same external solution as in perforated whole-cell recording. The pipette contained the same external solution with 25 μM glutamate added. Holding potential was 0mv. The other recording conditions were the same as in perforated whole-cell recording. For display and analysis, the signal was resampled at 5 kHz and filtered at 100 Hz by an 8 pole low-pass Bessel filter.

Neurotoxicity studies

Apoptosis was induced in neuronal cultures by stimulating the cells either with glutamate (75 μM) or a combination of gp120 (100 pM) and glutamate (25 μM). This involved washing the cells twice with a salt solution consisting of (in mM): 120 NaCl, 5.4 KCl, 10 $CaCl_2$, 25 Tris·HCl, 15 glucose, adjusted to pH 7.4 with NaOH, followed by a 15 min incubation of the cells with the gp120 and glutamate with or without CALP or control compounds at the specific concentrations. After stimulation, the cells were washed twice more in the control salt solution; fresh media warmed to 37°C was replaced and the cells were returned to the 37°C incubator for 20–24 h.

Cell death was determined in these experiments by using fluorescein diacetate and propidium iodide staining (34–36). Cultures were washed twice with Hanks' balanced salt solution (HBSS), then incubated with fluorescein diacetate (4 μM) and propidium iodide (36 μM) in HBSS for 3 min at room temperature. This was followed by a quick wash with HBSS and the cells were then viewed using a Nikon Diaphot 200 inverted epifluorescence microscope (Japan) with a 20× objective. An average of five microscope fields containing ~75 cells per field were counted from each well. Each condition was repeated in at least three different wells; thus, the total cells counted for each data point is ~1100 cells. The graph shows the mean of these triplicates ± SE.

To specifically measure apoptosis in these cells, the TUNEL method was used (37). First the cells were briefly fixed with Bouin's solution (Sigma) and permeabilized with phosphate-buffered saline (PBS)/1% Tween 20. The TUNEL method involves labeling the nicked DNA (a characteristic of apoptotic cells) with biotin-16-dUTP and subsequently with alkaline phosphatase (Boehringer Mannheim, Indianapolis, Ind.), and developed using Fast Red (Sigma). The cells were then viewed on a light microscope (Zeiss) using a 20× objective and counted as for the FDA/PI experiments. Similar numbers of cells were counted as for the FDA/PI experiment and are represented as mean ± SE.

Lymphocytotoxicity studies

Apoptosis was induced in ~3×10^5 peripheral blood mononuclear cells by the addition of 5 μg/ml native gp120 (Advanced Biotechnologies Inc., Columbia, Md.), 3 μg/ml superantigen mixture (consisting of 1 μg/ml of each Staphylococcal enterotoxin A and B, and toxic shock syndrome toxin-1; Sigma) or 10 μM dexamethasone in the RPMI media. CALP (100 μM) was added in the specified conditions. After 24 h of incubation at 37°C, the cells were washed with PBSAz (PBS containing 2% fetal calf serum and 0.01% sodium azide). Cells were then pelleted and resuspended in 20 μg/ml of 7-amino actinomycin D (7AAD; Sigma) in PBSAz and incubated at 4°C for 20 min. The cells analyzed by flow cytometry on a Becton Dickinson FACSCalibur (Mountain View, Calif.). Each condition was done in triplicate and graphed as mean ± SE.

RESULTS

CALP is readily taken up by cells

Since the putative site of interaction for the CALP peptides is located within the cytoplasm, it was necessary to test whether these peptides would be

able to enter cells. A modified version of CALP1 (see F-CALP1 in Table 1) was conjugated to fluorescein malemide so that it could be visualized by fluorescent microscopy. F-CALP rapidly entered rat neocortical neuronal cultures (**Fig. 1*A, B***) or Jurkat T cells (Fig. 1*C*), resulting in staining throughout the cytoplasm. A hydrophilic control peptide of the same size and conjugated to fluorescein malemide (see F-MBP in Table 1) did not enter the cells (Fig. 1*D*). This demonstrates that the fluorescein malemide is not responsible for uptake of the CALP peptide by the cells.

Further evidence that the CALP peptides can enter the cells comes from several electrophysiological studies discussed below. The most striking of these come from recordings done in the cell-attached configuration, in which the channels being recorded are separated from the bath by the giga ohm seal of the pipette. Addition of CALP to the extracellular bath results in these channels being blocked, which demonstrates the ability of the peptide to enter the cell and diffuse to the site of action.

CALP is a Ca^{2+} channel blocker

The first approach we took to examine whether CALP could inhibit Ca^{2+} entry used the ratiometric Ca^{2+} indicator dye, Fura-2. Cultured rat neocortical neurons loaded with this dye were exposed to glutamate (75 μm) either in the presence or absence of CALP or controls (**Fig. 2**), and the resulting increase in the cytoplasmic free Ca^{2+} concentration ($[Ca^{2+}]_i$) was measured. Given as a bolus, glutamate caused a large sustained increase in $[Ca^{2+}]_i$, (Fig. 2*A*). This was inhibited by CALP1 and CALP3 in a dose-dependent manner (Fig. 2*C*; IC_{50}=54.43±2.767 μM and 37.25±2.585 μM, respectively). Cyclizing CALP3 abolishes its ability to interact with EF hands of CaM (33). Consequently, cyclic CALP3 was unable to inhibit Ca^{2+} influx, and this peptide served as a negative control. Since the majority of Ca^{2+} channels activated by glutamate in these cells are of the N-methyl-D-aspartate (NMDA) type, the specific antagonist to these channels, MK801, was an effective positive control (IC_{50}=51.26±6.368 μM) (38). The ability of the CaM antagonist N-(6-aminohexyl)-5-chloro-1-naphthalenesulfonamide (W-7) to abolish the inhibitory effect of CALP and restore a large measure of the response of these cells to glutamate(Fig. 2*D*) demonstrates that the mode of action of these peptides is different from MK801 and involves CaM as an intermediary.

To study the actual channel activity involved in this process, we used patch clamping techniques. **Figure 3** shows a recording done in the perforated whole-cell configuration of rat neocortical neurons. When glutamate (25 μM) is applied to the bath, a large inward conductance is activated. Subsequent appli-

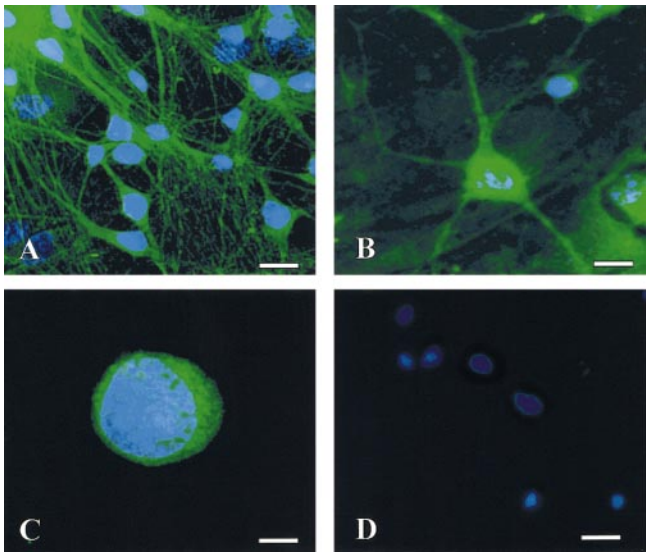

Figure 1. Fluorescent microscopic images of cells loaded with F-CALP1. Cultured rat neocortical neurons (*A, B*) or Jurkat T cells (*C*) stained with F-CALP1 both showed diffuse cytoplasmic staining (green) throughout the cell. Cells were counterstained with Hoechst 33258 (7.5 μM, blue color) to show the nuclei of cells. No cytoplasmic staining was noticed with the fluorescein-labeled hydrophilic control peptide, F-MBP (*D*). White bars on (*A–D*) represent 10, 4, 4, and 10 μm, respectively.

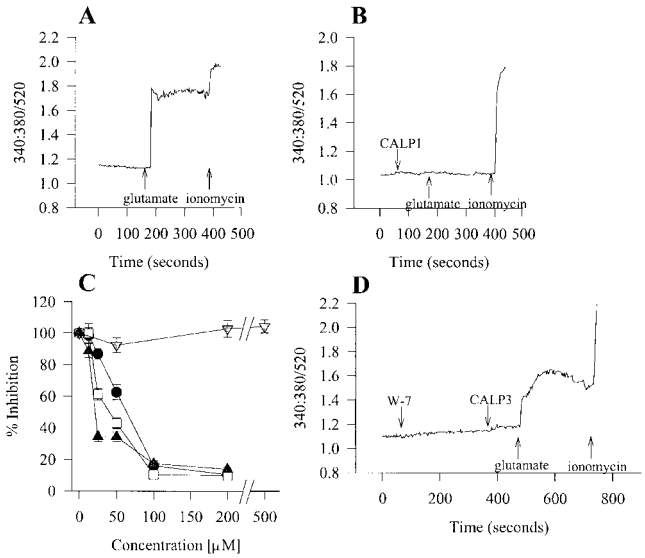

Figure 2. Inhibition of glutamate-induced $[Ca^{2+}]_i$ increase by CALP1 in rat neocortical neurons. *A)* Fura-2-loaded neuronal cultures were stimulated with glutamate (75 μM), which caused a substantial increase in $[Ca^{2+}]_i$. Ionomycin (10 μM) was added at the end of the experiment to check for proper loading and whether the signal was in the limits of saturation of the dye. Shown here is an average of 20 cells from one coverslip. *B)* Addition of CALP1 (100 μM) prior to glutamate stimulation prevented the increase in $[Ca^{2+}]_i$. Once again, ionomycin was added at the end of the experiment. *C)* This inhibition was dose dependent for CALP1 (●), CALP3 (□), and MK801 (▲), but cyclic CALP3 (▼) did not inhibit this response at all. *D)* Exposure to W-7 (5 μM) prior to CALP3 (100 μM) restores the responsiveness of these cells to glutamate (75 μM).

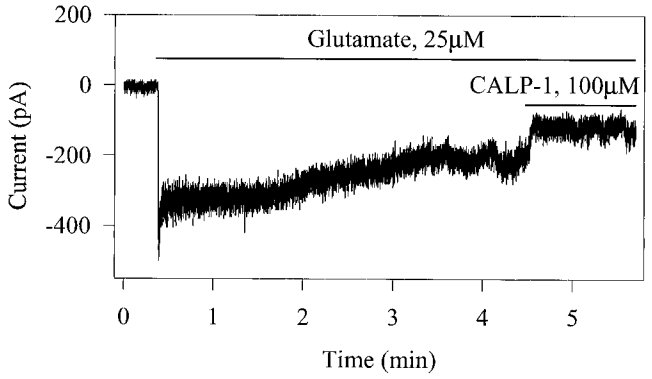

Figure 3. Inhibition of glutamate-induced current by CALP1 in cultured rat neocortical neurons measured by patch clamping. Current trace of neuron in perforated whole-cell configuration held at −80 mV. On perfusion of the cell with glutamate (25 μM), a large current is induced. Subsequent perfusion of the cell by glutamate (25 μM) plus CALP1 (100 μM) dramatically decreases this current almost to baseline levels.

cation of 100 μM CALP1 to the chamber almost completely blocked the current. However, CALP1 had little effect on glutamate-induced current in conventional whole-cell configuration (data not shown). This suggests that the inhibition of glutamate-induced current by CALP1 is dependent on a diffusible factor, such as CaM, which was washed out rapidly during conventional whole-cell recording. To confirm that CALP1 acted on glutamate-induced currents by interacting with a binding site in the cytoplasm, we recorded from these cells in the cell-attached mode. In this instance, glutamate (25 μM) was placed in the pipette solution, activating multiple channels in this patch (**Fig. 4**). Each of these opened channels had a single-channel conductance of 50–70 pS, suggesting it was predominantly carried by the NMDA receptor. Application of 100 μM CALP1 to the bath reversibly blocked the NMDA currents (Fig. 4). CALP1 blockage of the NMDA

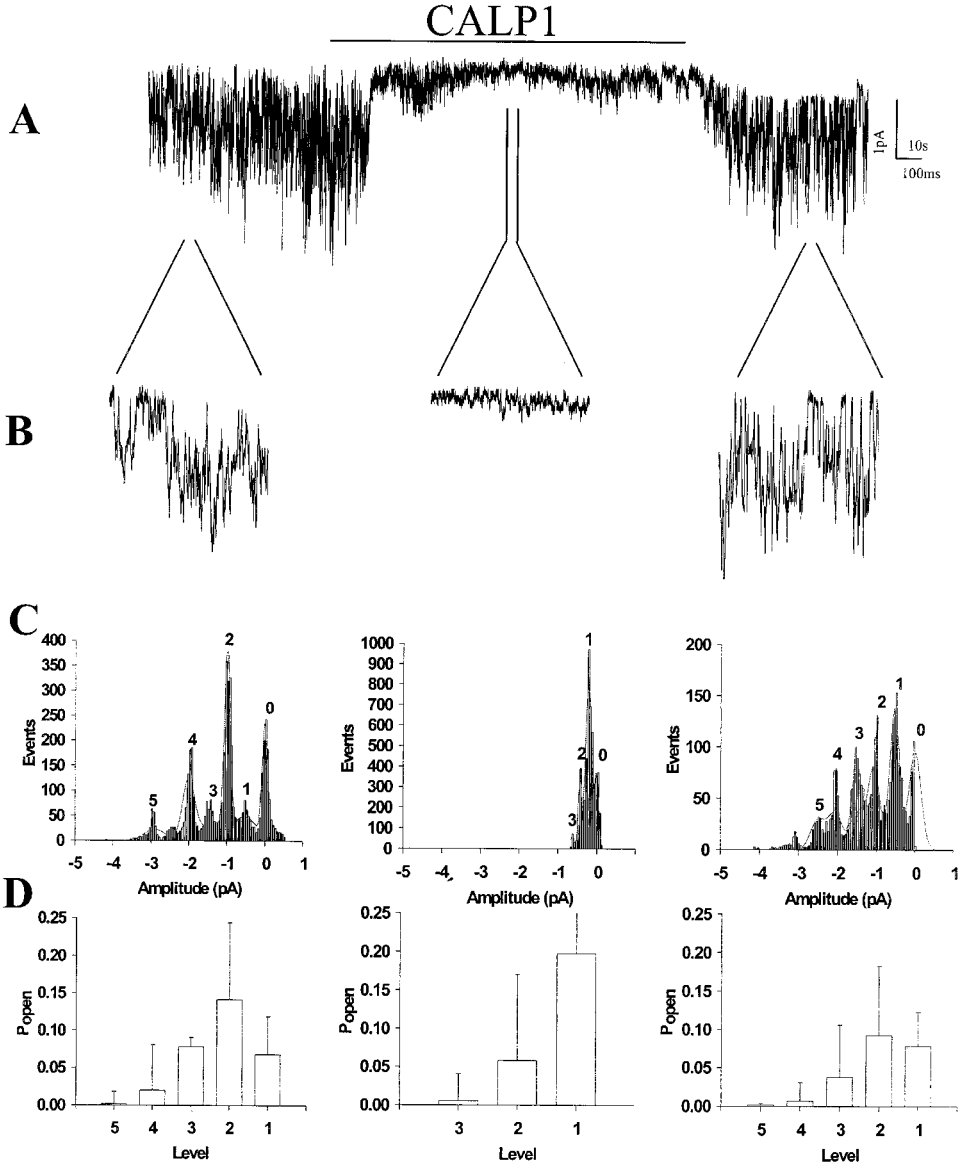

Figure 4. *A, B)* Single-channel activity in cell-attached mode of glutamate (25 μM, in pipette solution) -induced current shows multiple channel openings when the cell is perfused with control solution. Perfusing the cell with CALP1 (100 μM) containing solution markedly blocks the channel activity after a short delay. Washing the CALP1 away from the cell with control solution reinstates the glutamate-induced current. *B)* Representative segments of the trace in panel *A* on an expanded time scale. Analysis of these segments shows the effect of CALP1 on both the single-channel conductance (*C*) as well as the open probability (*D*).

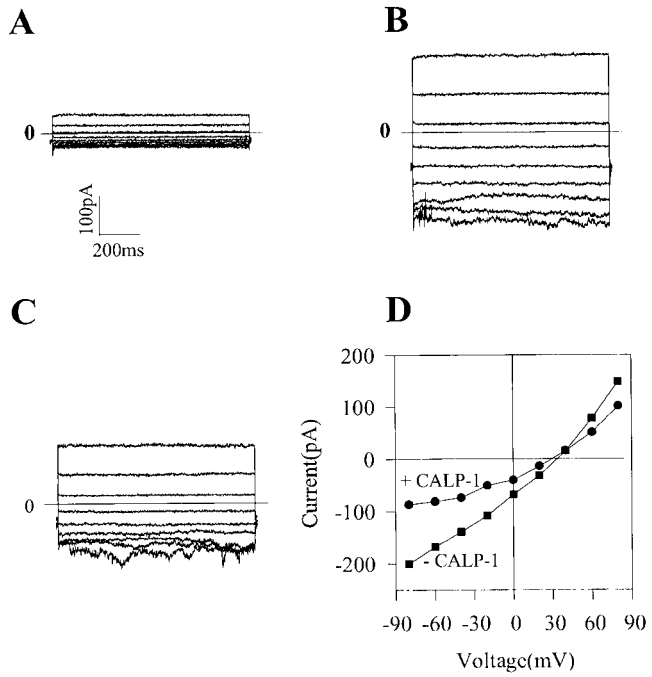

Figure 5. I_{NSCC} activated by gp120 in Jurkat T cell is blocked by CALP1. I_{NSCC} is recorded as described in Materials and Methods. Representative traces of whole-cell currents before the addition of gp120 (*A*), 2.5 min after the addition of gp120 (100 pM) (*B*), and 2 min after the addition of CALP1 (40 μM) (*C*). *D)* The I-V relationship of the currents shown in panels *B, C* after the leak currents shown in panel *A* were subtracted. I_{NSCC} is characterized by large noise of the currents, a reversal potential around 30 mV, and an outwardly rectified pattern.

current in the cell-attached mode demonstrates that the peptide was able to gain access to the interior of the cell. Furthermore, the reversibility of the glutamate-induced current after the CALP was washed from the bath solution demonstrates that the peptide did not accumulate in the pipette. Therefore, we concluded that CALP1 blocked the NMDA receptor by acting on the cytoplasmic side. Single-channel analysis of the inhibition caused by CALP1 revealed that the effect was partially due to a decrease in the single-channel conductance (Fig. 4*C*) as well as a decrease in the open probability (Fig. 4*D*).

It has been demonstrated that the HIV-1 envelope glycoprotein, gp120, can cause a Ca^{2+} influx in $CD4^+$ T cells due to an interaction with the chemokine receptor, CCR5 (39). We found that gp120 can activate a nonselective cation channel (I_{NSCC}) in Jurkat cells, which is permeable to Ca^{2+}. We tested the effects of CALP1 on this channel. As shown in **Fig. 5**, addition of 8.3 nM gp120 activated a large, outwardly rectified conductance with a reversal potential of around 30 mV, indicating it was carried by a nonselective cation channel. Addition of 40 μM CALP1 blocked 60% of the current (Fig. 5*C*). This blockage is also demonstrated on isolated patch recordings in the inside-out configuration, demonstrating a direct effect of the peptide on the channel (**Fig. 6**). In contrast to the effect of the peptide on glutamate receptor channels, single-channel analysis reveals that the inhibitory effect of CALP1 on I_{NSCC} is due to the decrease of the open probability, but not the single-channel conductance (Fig. 6*C*). Furthermore, at equivalent concentrations of CALP, the blockage of these channels was greater on recordings done in the inside-out configuration (Fig. 6) than outside-out (data not shown). This provides further evidence that CALP is interacting with a target on the cytoplasmic face of the channel.

CALP inhibits apoptosis

Glutamate is the major excitatory amino acid used in the central nervous system, but if the concentration becomes too high (for example, in ischemic conditions) it can result in significant cytotoxicity (5, 6, 40). This provided an excellent model for studying the possible anti-apoptotic effects of CALP, since this process of cell death is dependent on the sustained increase in $[Ca^{2+}]_i$ due to the opening of glutamate receptor channels. Cultured rat neocortical neurons were exposed to glutamate (75 μM) either in the presence or absence of CALP or control substances for 15 min, then washed with fresh media and incubated overnight. Cytotoxicity (**Fig. 7*A***) was measured by staining the cells with fluorescein diacetate, which live cells take up and cleave resulting in green fluorescence, and propidium iodide, which dead cells take up resulting in red fluorescence (34–36). CALP1 and CALP3 were able to inhibit this cytotoxicity in a dose-dependent manner (IC_{50}= 52.48±1.651 μM, IC_{50} =50.97±1.583 μM, respectively), as was MK801. Apoptosis (Fig. 7*B*) was also measured in this system by using the TUNEL method (37) to stain nuclei of the cells with cleaved DNA, which is characteristic of apoptosis. CALP's dose-dependent inhibition of apoptosis in this system (CALP1 IC_{50}=44.78±0 μM, CALP3 IC_{50} =33.41±1.099 μM) was similar not only to the cytotoxicity measurements, but also to the Fura-2 imaging studies. This suggests that the inhibition of apoptosis is mainly due to the inhibition of the influx of Ca^{2+}. This ability of Ca^{2+} channel blockers to inhibit cytotoxicity has been shown previously and is further supported by the action of MK801 in this system. Once again, cyclic CALP3 did not inhibit the effect of glutamate.

In another system, we studied the anti-apoptotic effects of CALP in a well-characterized model of HIV neurotoxicity in cultured rat neocortical cells. The HIV-1 envelope glycoprotein gp120 (100 pM), in addition to a relatively small amount of glutamate (25 μM), induces a rapid apoptotic effect that is known to be dependent on the influx of Ca^{2+}

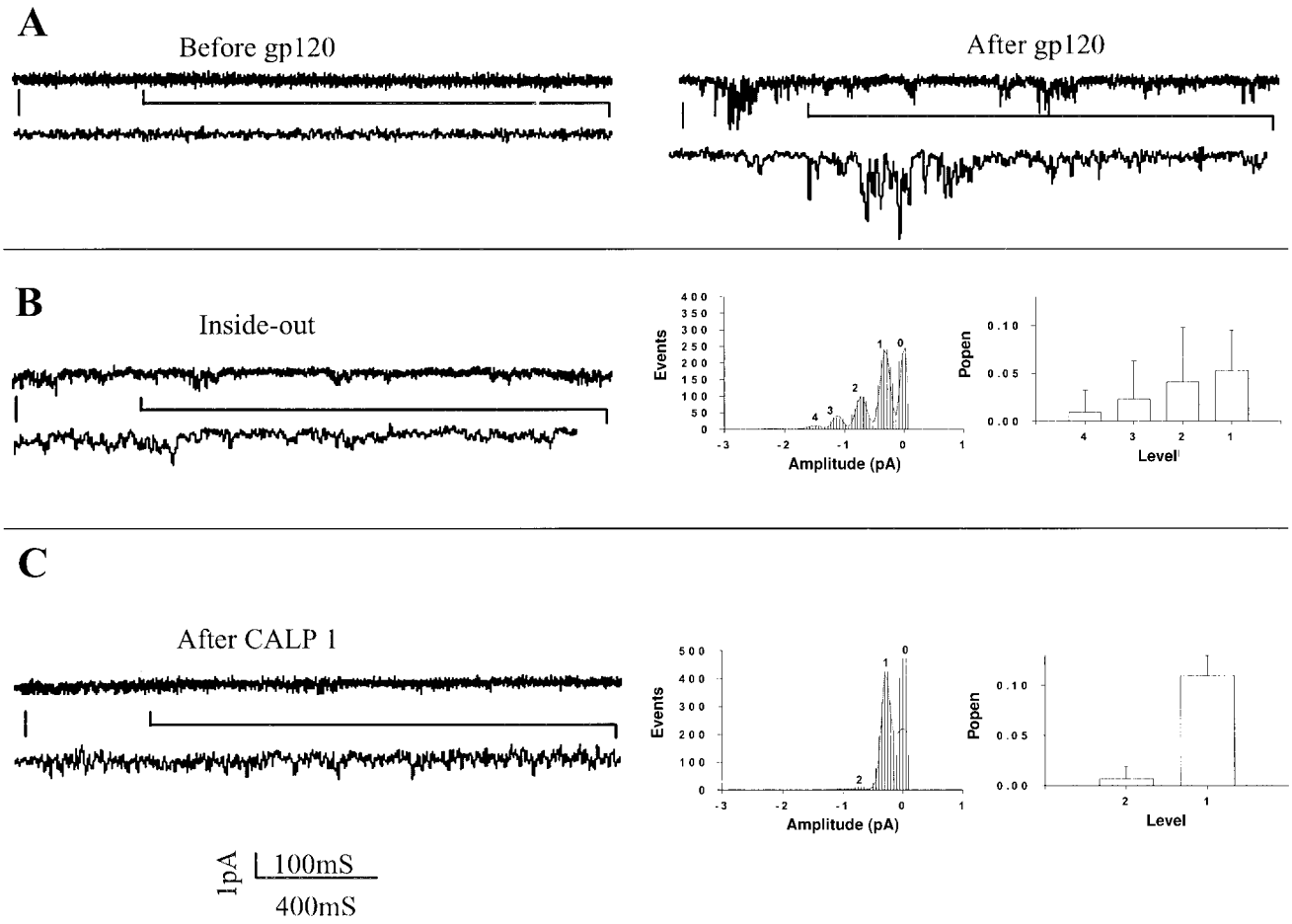

Figure 6. Single-channel activity of I_{NSCC} activated by gp120 *A)* in cell-attached mode, *B)* after the excision of the patch, and *C)* after perfusion of the intracellular face of the patch with CALP1-containing solution. Single-channel analysis (*B, C*) shows that the inhibitory effect of CALP1 on this channel is mediated through a decrease in open probability, but not channel conductance. Bottom traces show section from top trace, indicated by bars, on an expanded time scale.

through glutamate receptor channels (7–9, 41–45). In contrast to the glutamate excitotoxicity model described above, the combination of these two compounds results in cytotoxicity that is mostly due to apoptosis. As shown in **Table 2**, CALP1 (30 μM) was as effective at inhibiting apoptosis in this system as the combination of NMDA-R and non-NMDA-R blockers (10 μM MK801 and 100 μM DNQX, respectively) or even the omission of Ca^{2+} from the extracellular media during stimulation. Other positive controls known to inhibit this type of apoptosis are the L-type Ca^{2+} channel blocker nifedipine (100 μM), as well as an agent, dantrolene (30 μM), which is known to inhibit the release of Ca^{2+} from internal stores (40).

HIV causes apoptosis in uninfected $CD4^+$ T cells by an as yet unknown mechanism. It is known, however, that the engagement of the CD4 receptor by gp120, followed by stimulation of the T cell receptor (TCR) complex, can lead to apoptosis of these cells (46–50). Therefore, we induced apoptosis in T cell-enriched human peripheral blood lympho-

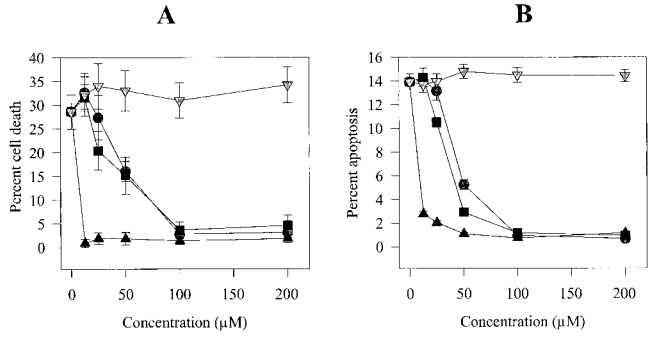

Figure 7. Inhibition of glutamate (75 μM) -induced neurotoxicity in cultured rat neocortical neurons. CALP1 (gray filled circle) and CALP3 (■) inhibited the toxic effects of glutamate in these cultures as did MK801 (gray filled triangle), whereas cyclic CALP3 (gray filled inverted triangle) had no effect. *A)* Cell death was measured by staining cells with fluorescein diacetate, which is taken up by live cells and cleaved, resulting in green fluorescence, and propidium iodide, which is taken up by dead cells and makes them fluorescent red. *B)* Apoptosis was specifically measured by staining the cells using the TUNEL method.

TABLE 2. *Inhibition of gp120 mediated neurotoxicity by CALP and glutamate receptor antagonists as well as calcium channel blockers*[a]

	Cell death, %	Apoptosis, %
Control	3.6 ± 1.5*	4.8 ± 2.7*
gp120 (100 pM)	7.2 ± 2.4*	6.1 ± 3.0*
Glutamate (25 μM)	13.3 ± 5.7*	7.1 ± 3.3*
gp120 (100 pM)		
+ glutamate (25 μM)	39.5 ± 5.7	40.0 ± 9.3
+CALP1 (30 μM)	7.3 ± 1.8*	6.0 ± 2.6*
+cyclicCALP3 (30 μM)	45.3 ± 5.2	41.5 ± 6.7
+MK801 (10 μM)	22.8 ± 2.1*	21.0 ± 3.4*
+DNXQ (100 μM)	21.0 ± 2.9*	20.0 ± 3.8*
+Ca^{2+} free media	5.0 ± 2.3*	3.6 ± 1.1*
+ MK801 (10 μM)		
+ DNQX (100 μM)	8.1 ± 2.5*	7.3 ± 3.2*
+Nifedipine (100 μM)	6.5 ± 3.1*	12.6 ± 12.5*
+Dantrolene (30 μM)	5.7 ± 2.4*	4.7 ± 2.3*

[a] Data are means ± standard deviation ($n = 15$). Cell death was measured by fluorescein diacetate/propidium iodide staining, apoptosis was measured by TUNEL staining. Significant differences from gp120 + glutamate condition were determined by Mann-Whitney U test, * $P < 0.001$.

cytes using a system whereby the cells are exposed to gp120 prior to superantigen stimulation of the TCR. After 24 h incubation, the cells were stained with 7AAD and analyzed by flow cytometry. Loss of membrane integrity leading to the uptake of this dye, together with a decrease in cell size, are the two characteristics of apoptosis measured by this procedure (51). As **Fig. 8** shows, gp120 and a superantigen mixture have a synergistic effect on these cells, resulting in a much larger apoptotic signal than the combined effect of each reagent separately. However, if either CALP1 or CALP3 (100 μM) is present beforehand, then this signal and the resulting apoptosis can be inhibited. One again, cyclic CALP3 did not inhibit this cytotoxic process at all. Not all apoptosis is dependent on an initial influx of Ca^{2+}. One example of this is induced by dexamethasone. This compound causes a signal leading to apoptosis by direct interaction with the glucocorticoid receptor leading to DNase I susceptibility (52–54). The fact that CALP did not inhibit apoptosis induced by dexamethasone demonstrates that the peptide is acting as an anti-apoptotic agent through its channel blocking activity, and not some downstream effector.

DISCUSSION

Since Ca^{2+} is a potent second messenger within the cytoplasm, its distribution must be tightly regulated. Therefore, cells use many different strategies for buffering, storage, and transport of this cation. Hence, many Ca^{2+}-permeable channels have Ca^{2+}-dependent mechanisms to negatively feedback their activity. This regulation can either be direct, by having Ca^{2+} binding domains within the cytoplasmic regions of the channel itself, or indirect, mediated through the effects of a Ca^{2+} binding protein such as CaM. Often channels use more than one mechanism to regulate its Ca^{2+} permeability. For example, the NMDA receptor has been shown to be inactivated through direct binding of CaM and also by several other proteins in a Ca^{2+}-dependent manner (19–25). Although the NSCC channel mentioned above has not been cloned, we have observed a negative feedback regulated by Ca^{2+} (unpublished observations); however, more work needs to be done to elucidate the exact mechanism by which this occurs.

We have previously demonstrated that CALP1 and CALP3 mimic the effect of Ca^{2+} through their specific interaction with EF hands (32, 33). We have shown that they bind to CaM in the carboxyl-terminal Ca^{2+} binding sites, and this interaction results in a conformational change whereby the CALP/CaM complex can activate phosphodiesterase in the absence of Ca^{2+}. In this study we have extended our investigations to show the biological relevance of designing such peptides. Specifically, these peptides represent a new class of Ca^{2+} channel blocker that

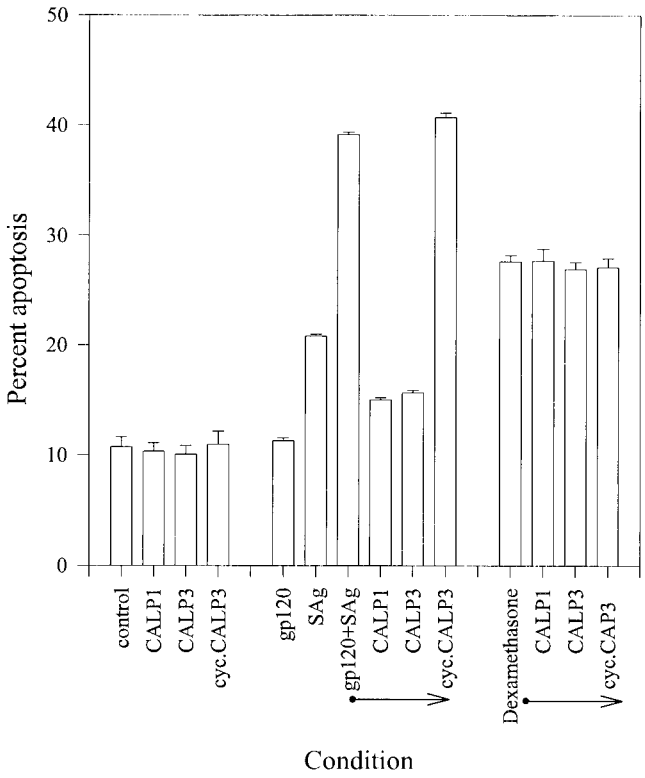

Figure 8. Inhibition of apoptosis induced by HIV gp120 and SAg in Human T cells by CALP. Apoptosis was measured by staining the cells with 7AAD and analyzing them by flow cytometry. The combination of gp120 (5 μg/ml) and SAg cocktail (3 μg/ml) induced apoptosis after 24 h incubation over and above each of these alone. CALP1 (100 μM) and CALP3 (100 μM) inhibited this, whereas cyclic CALP3 (100 μM) did not. Dexamethasone (10 μM) -induced apoptosis was not affected by any of the CALP peptides.

exert their action not on the pore regions of the channel or the ligand binding sites of certain receptor channels, but rather on the Ca^{2+} sensing mechanisms. Depending on the channel, this inhibitory effect can be mediated through a direct interaction of the peptide with the cytoplasmic face of the channel, as demonstrated with the NSCC, or it can be indirect—mediated through CaM, as demonstrated with the glutamate receptor channels. The different mechanisms of interaction of the peptide with the channels were also demonstrated by the distinct changes produced in the single-channel properties.

As a consequence of the channel blocking ability of these peptides, apoptosis mediated by an influx of Ca^{2+} through these channels was also inhibited. This inhibition was demonstrated to be specific, since neither CALP1 nor CALP3 were able to inhibit dexamethasone-induced apoptosis. Given the importance of apoptosis mediated by a Ca^{2+} influx in many disease processes, some of which have been modeled here, these peptides could be useful lead products for the design of therapeutic agents to interfere with such cytotoxicity.

Furthermore, since Ca^{2+} plays a role in other signaling processes apart from the induction of apoptosis, CALP may also be useful in their modulation. We have observed the effect of CALP on the contraction of urinary smooth muscle (32) and canine heart muscle (our unpublished observation). Another Ca^{2+}-mediated process is airway hyperresponsiveness, which can be modeled as the constriction of isolated guinea pig trachea perfused with acetylcholine or histamine. Nitric oxide (NO) is normally produced by the epithelia surrounding the lumen of the trachea in a Ca^{2+}-dependent manner, which acts as an important feedback mechanism against bronchoconstriction induced by histamine or cholinergic receptor agonists. We have observed the modulation of the histamine or acetylcholine-induced constriction of isolated guinea pig trachea by CALP (unpublished results). This demonstrates the ability of these peptides to modulate Ca^{2+}-mediated signaling pathways apart from those involved in a cytotoxic response.

In a more general sense, by using the design principles for CALP, it may be possible to produce peptides to interact with other ion channels in a more specific and targeted manner. With the continuing elucidation of channel structure and function, from pore regions to gating mechanisms and other regulatory domains, come further opportunities for such design. We have also demonstrated with the CALP series the ability to design peptides to interact with the same region on CaM with opposing action (33). This suggests that it may be possible not only to regulate distinct types of ion channels, but to regulate them in opposing ways. Certainly this could lead to many new and specific channel agonists and antagonists that would have great benefit in a vast number of disease processes. FJ

Thanks to Diane Wiegent for editorial assistance in the preparation of this manuscript. This work was supported by grants to J.E.B. from the National Institutes of Health (MH 52527, AI 37670, and NS 29719) and to Lisa Coplan and Chad Constance for technical assistance with peptide synthesis.

REFERENCES

1. Berridge, M. J., Bootman, M. D., and Lipp, P. (1998) Calcium—a life and death signal. *Nature (London)* **395,** 645–648
2. Susin, S. A., Zamzami, N., and Kroemer, G. (1998) Mitochondria as regulators of apoptosis: doubt no more. *Biochim. Biophys. Acta* **1366,** 151–165
3. McConkey, D. J. (1996) The role of calcium in the regulation of apoptosis. *Scanning Microsc.* **10,** 777–793
4. Trump, B. F., and Berezesky, I. K. (1995) Calcium mediated cell injury and cell death. *FASEB J.* **9,** 219–228
5. Lei, S. Z., Zhang, D., Abele, A. E., and Lipton, S. A. (1992) Blockage of NMDA receptor-mediated mobilization of intracellular Ca^{2+} prevents neurotoxicity. *Brain Res.* **598,** 196–202
6. Hahn, J. S., Aizenman, E., and Lipton, S. A. (1988) Central mammalian neurons normally resistant to glutamate toxicity are made sensitive by extracellular Ca^{2+}: toxicity is blocked by the N-methyl-D-aspartate antagonist MK801. *Proc. Natl. Acad. Sci. USA* **85,** 6556–6560
7. Dreyer, E. B., Kaiser, P. K., Offermann, J. T., and Lipton, S. A. (1990) HIV-1 coat protein neurotoxicity prevented by calcium channel antagonists. *Science* **248,** 364–367
8. Savio, T., and Levi, G. (1993) Neurotoxicity of HIV coat protein gp120, NMDA receptors, and protein kinase C: a study with rat cerebellar granule cell cultures. *J. Neurosci. Res.* **34,** 265–272
9. Dawson, V. L., Dawson, T. M., Uhl, G. R., and Snyder, S. H. (1993) Human immunodeficiency virus type 1 coat protein neurotoxicity mediated by nitric oxide in primary cortical cultures. *Proc. Natl. Acad. Sci. USA* **90,** 3256–3259
10. DeLeon, M., Wang, Y., Jones, L., Perez Reyes, E., Wei, X., Soong, T. W., Snutch, T. P., and Yue, D. T. (1995) Essential Ca^{2+}-binding motif for Ca^{2+} sensitive inactivation of L-type Ca^{2+} channels. *Science* **270,** 1502–1506
11. Yue, D. T., Backx, P. H., and Reuter, H. (1990) Ca^{2+} sensitive inactivation of L-type Ca^{2+} channels in the gating of single calcium channels. *Science* **250,** 1735–1738
12. Sherman, A., Keizer, J., and Rinzel, J. (1990) Domain model for Ca^{2+}-interaction of Ca^{2+} channels at low channel density. *Biophys. J.* **58,** 985–995
13. Zuhkle, R. D., and Reuter, H. (1998) Ca^{2+} sensitive inactivation of L-type Ca^{2+} channels depends on multiple cytoplasmic amino acid sequences of the alpha 1C subunit. *Proc. Natl. Acad. Sci. USA* **95,** 3287–3294
14. Haack, J. A., and Rosenberg, R. L. (1994) Calcium-dependent inactivation of L-type Ca^{2+} channels in planar lipid bilayers. *Biophys. J.* **66,** 1051–11060
15. Peterson, B. Z., Lee, J. S., Mulle, J. G., Wang, Y., DeLeon, M., and Yue, D. T. (1999) Individual amino acids within a consensus EF-hand motif are critical for calcium-dependent inactivation of α_{1C} calcium channels. *Biophys. J.***76,** A340 (abstr.)
16. Qin, N., Olcese, R., Bransby, M., Lin, T., and Birnbaumer, L. (1999) Ca^{2+}-induced inhibition of the cardiac Ca^{2+} channel depends on calmodulin. *Proc. Natl. Acad. Sci. USA* **96,** 2435–2438
17. Grunwald, M. E., Yu, W. P., Yu, H. H., and Yau, K. W. (1998) Identification of a domain on the β-subunit of the rod cGMP-gated cation channel that mediates inhibition by calcium-calmodulin. *J. Biol. Chem.* **273,** 9148–9157
18. Fanger, C. M., Ghanshani, S., Logsdon, N. J., Rauer, H., Kalman, K., Zhou, J., Beckingham, K., Chandy, K. G., Cahalan, M. D., and Aiyar, J. (1999) Calmodulin mediates calcium-dependent acti-

vation of the intermediate conductance K_{Ca} channel, *IKCa1*. *J. Biol. Chem.* **274,** 5746–5754
19. Krupp, J. J., Vissel, B., Thomas, C. G., Heinemann, S. F., and Westbrook, G. L. (1999) Interactions of calmodulin and α-actinin with the NR1 subunit modulate Ca^{2+}-dependent inactivation of NMDA receptors. *J. Neurosci.* **19,** 1165–1178
20. Levitan, I. B. (1999) It is calmodulin after all: Mediator of the calcium modulation of multiple ion channels. *Neuron* **22,** 645–648
21. Zhang, S., Ehlers, M. D., Berndardt, J. P., Su, C. T., and Huganir, R. L. (1998) Calmodulin mediates calcium-dependent inactivation of N-methyl-D-aspartate receptors. *Neuron* **21,** 443–453
22. Wyszynski, M., Lin, J., Rao, A., Nigh, E., Beggs, A. H., Craig, A. M., and Sheng, M. (1997) Competitive binding of α-actinin and calmodulin to the NMDA receptor. *Nature (London)* **385,** 439–442
23. Ehlers, M. D., Zhang, S., Bernhardt, J. P., and Huganir, R. L. (1996) Inactivation of NMDA receptors by direct interaction of calmodulin with the NR1 subunit. *Cell* **84,** 745–755
24. Rosenmund, C., and Westbrook, G. L. (1993) Calcium-induced actin depolymerization reduces NMDA channel activity. *Neuron* **10,** 805–810
25. Armstrong, D. L. (1989) Calcium channel regulation by calcineurin, a Ca^{2+}-activated phosphatase in mammalian brain. *Trends Neurosci.* **12,** 117–122
26. Phillips, A. M., Bull, A., and Kelly, L. E. (1992) Identification of a Drosophila gene encoding a calmodulin-binding protein with homology to the *trp* phototransduction gene. *Neuron* **8,** 631–642
27. Warr, C. G., and Kelley, L. E. (1996) Identification and characterization of two distinct calmodulin-binding sites in the trpl ion-channel protein of *Drosophila melanogaster*. *Biochem. J.* **314,** 497–503
28. Estacion, M., Sinkins, W. G., and Schilling, W. P. (1999) Stimulation of *Drosophila* trpL by capacitative Ca^{2+} entry. *Biochem. J.* **341,** 41–49
29. Gardner, P., Alcover, A., Kuno, M., Moingeon, P., Weyand, C. M., Goronzy, J., and Reinherz, E. L. (1989) Triggering of T-lymphocytes via either T3-Ti or T11 surface structures opens a voltage-insensitive plasma membrane calcium-permeable channel: requirement for interleukin-2 gene function. *J. Biol. Chem.* **264,** 1068–1076
30. Blalock, J. E. (1995) Genetic origins of protein shape and interaction rules. *Nature Med.* **1,** 876–878
31. Baranyi, L., Campbell, W., Oshima, K., Fujimoto, S., Boros, M., and Okada, H. (1995) The antisense homology box: a new motif within proteins that encodes biologically active peptides. *Nature Med.* **1,** 894–901
32. Dillon, J., Woods, W. T., Guarcello, V., LeBoeuf, R. D., and Blalock, J. E. (1991) A peptide mimetic of calcium. *Proc. Natl. Acad. Sci. USA* **88,** 9726–9729
33. Villain, M., Jackson, P. L., Manion, M. K., Su, Z., Fassina, G., Johnson, T. M., Sakai, T. T., Krishna, N. R., and Blalock, J. E. (2000) De novo design of peptides targeted to the EF hands of calmodulin. *J. Biol. Chem.* **274,** 2676–2685
34. Darzynkiewcz, Z., Li, X., and Gong, J. (1994) Assays of cell viability: discrimination of cells dying by apoptosis. *Methods Cell Biol.* **41,** 15–38
35. Keilhoff, G., and Wolf, G. (1993) Comparison of double fluorescence staining and LDH-test for monitoring cell viability in vitro. *NeuroReport* **5,** 129–132
36. Altman, S. A., Randers, L., and Rao, G. (1993) Comparison of trypan blue dye exclusion and fluorometric assays for mammalian cell viability determinations. *Biotechnol. Prog.* **9,** 671–674
37. Gavrieli, Y., Sherman, Y., and Ben-Sasson, S. A. (1992) Identification of programmed cell death in situ via specific labelling of nuclear DNA fragmentation. *J. Cell Biol.* **119,** 493–501
38. Woodruff, G. N., Foster, A. C., Gill, R., Kemp, J. A., Wong, E. H., and Iversen, L. L. (1987) The interaction between MK-801 and receptors for N-methyl-D-aspartate: functional consequences. *Neuropharmacology* **26,** 903–909
39. Weissman, D., Rabin, R. L., Arthos, J., Rubbert, A., Dybul, M., Swofford, R., Venkatesan, S., Farber, J. M., and Fauci, A. S. (1997) Macrophage-tropic HIV and SIV envelope proteins induce a signal through the CCR5 chemokine receptor. *Nature (London)* **389,** 981–985
40. Frandsen, A., and Schousboe, A. (1992) Mobilization of dantrolene-sensitive calcium pools is involved in the cytotoxicity induced by quisqualate and N-methyl-D-aspartate but not by 2-amino-3-(3-hydroxy-5-methylisoxazol-4-yl)propionate and kainate in cultured cerebral cortical neurons. *Proc. Natl. Acad. Sci. USA* **89,** 2590–2594
41. Lipton, S. A., Sucher, N. J., Kaiser, P. K., and Dreyer, E. B. (1991) Synergistic effects of HIV coat protein and NMDA receptor mediated neurotoxicity. *Neuron* **7,** 111–118
42. Kaiser, P. K., Offerman, J. T., and Lipton, S. A. (1990) Neuronal injury due to HIV-1 envelope protein is blocked by anti-gp120 but nor by anti-CD4 antibodies. *Neurology* **40,** 1757–1761
43. Gougeon, M-L., and Montagnier, L. (1993) Apoptosis in AIDS. *Science* **260,** 1269–1270
44. Lipton, S. A. (1994) HIV-related neuronal injury. *Mol. Neurobiol.* **8,** 181–196
45. Diop, A. G., Lesort, M., Esclaire, F., Sindou, P., Couratier, P., and Hugon, J. (1994) Tetrodotoxin blocks HIV coat protein (gp120) toxicity in primary neuronal cultures. *Neurosci. Lett.* **165,** 187–190
46. Banda, N. K., Bernier, J., Kuahara, D. K., Kurrie, R., Haigwood, N., Sekaly, R., and Finkel, T. H. (1992) Crosslinking CD4 by human immunodeficiency virus gp120 primes T cells for activation-induced apoptosis. *J. Exp. Med.* **176,** 1099–1106
47. Groux, H., Torpier, G., Monte, D., Monton, Y., Capron, A., and Ameison, J. C. (1992) Activation induced death by apoptosis in $CD4^+$ cells from human immunodeficiency virus-infected asymptomatic individuals. *J. Exp. Med.* **175,** 331–340
48. Oyaizu, N., McCloskey, T. W., Than, S., Hu, R., and Pahwa, S. (1995) Mechanism of apoptosis in peripheral blood mononuclear cells of HIV-infected patients. In *Cell Activation and Apoptosis in HIV Infection* (Andrieu, J. M., and Lu, W., eds) Plenum Press, New York
49. Foster, S., Beverly, P., and Aspinall, R. (1995) gp120-induced programmed cell death in recently activated T cells without subsequent ligation of the T cell receptor. *Eur. J. Immunol.* **25,** 1778–1782
50. Tuosto, L., Montani, M. S. G., Lenzetti, S., Cundvi, E., Moertti, S., Lomabardi, G., and Piccolella, E. (1995) Differential susceptibility to monomeric HIV gp120 mediated apoptosis in antigen activated $CD4^+$ T cell populations. *Eur. J. Immunol.* **25,** 2907–2916
51. Philpott, N. J., Turner, A. J., Scopes, J., Westby, M., Marsh, J. C., Gordon-Smith, E. C., Dalgleish, A. G., and Gibson, F. M. (1996) The use of 7-amino acitnomycin D in identifying apoptosis: simplicity of use and broad spectrum of application compared with other techniques. *Blood* **87,** 2244–2251
52. Cidlowski, J. A., King, K. L., Evans-Storms, R. B., Montague, J. W., Bortner, C. D., and Hughes, F. M., Jr. (1996) The biochemistry and molecular biology of glucocorticoid-induced apoptosis in the immune system. *Recent Prog. Hormone Res.* **51,** 457–490
53. Bansal, N., Houle, A. G., and Melnykovych, G. (1990) Dexamethasone-induced killing of neoplastic cells of lymphoid derivation: lack of early calcium involvement. *J. Cell. Physiol.* **143,** 105–109
54. Bian, X., Hughes, F. M., Jr., Huang, Y., Cidlowski, J. A., and Putney, J. W., Jr. (1997) Roles of cytoplasmic Ca^{2+} and intracellular Ca^{2+} stores in induction and suppression of apoptosis in S49 cells. *Am. J. Physiol.* **272,** C1241–12499

Received for publication November 18, 1999.
Accepted for publication February 4, 2000.